IPPI
Polyolefins Journal, Vol. 11, No. 1 (2024)
DOI: 10.22063/POJ.2023.3412.1268
ORIGINAL PAPER

Effect of quenching temperature and filler rate on the mechanical thermal and physical properties of composites: Polypropylene/calcium carbonate

Leila Latreche[1,2], Samira Maou[3*], Lokmane-Taha Abdi[4] ,Tahir Habila[1,5], Yazid Meftah[1]

[1]Ecole Normale Supérieure de Boussaada, Boussaada 28201, Algeria
[2]Laboratory of Physical Chemistry of High Polymers, Ferhat Abbas University, Setif 1-Algeria19000
[3]Département de Chimie, Université Hassiba Ben Bouali de Chlef, Chlef 02180, Algeria
[4]Larbi Ben M'hidi Université, Oum El Bouaghi,-Algeria 4000
[5]Department of Chemistry, Laboratory of Phytochemistry and Pharmacology, University of Mohamed Seddik Benyahia, BP. 98,Ouled Aissa, Jijel, Algeria

Received: 6 August 2023, Accepted: 4 November 2023

ABSTRACT

Polypropylene (PP) is a strong, tough, crystalline thermoplastic material with high performance. Because of its diverse thermo-physical and mechanical properties, it is utilized in a wide variety of disciplines. In this study, the impact of free quenching on the thermo-physical characteristics of PP/calcium carbonate ($CaCO_3$) composites was examined. Three distinct heating procedures were used. First, composites were cooled from their melting phase temperature to ambient temperature. Second, composites were cooled from 130°C to a pre-determined and controlled temperature (T: 0°, 20°, 30°, 40°, 50°, 60°, 70°, 80°C). Third, composites were temperature-tested using annealing. The findings suggest that the elongation-at-break and impact strength may be improved following an initial quenching process from the melting phase to ambient temperature. On the other hand, a second quenching process at 0°C produces superior results, and a correlation between mechanical and thermal characteristics is noted; however, while these qualities are increased, others, such as flexibility, density, Vicat softening temperature (VST), and heat distortion temperature (HDT) are negatively impacted. **Polyolefins J (2024) 11: 11-19**

Keywords: Heat treatment; polypropylene; $CaCO_3$; thermal properties.

INTRODUCTION

Materials comprising PP, known for their excellent mechanical qualities, great corrosion resistance, and relatively inexpensive cost are utilized extensively in the automotive sector, packaging industry, and production of household goods [1-3]. As a result of the dispersion of fillers in the matrix, incorporating inorganic particles such as $CaCO_3$ can enhance the strength, electrical characteristics, thermal stability, and radiation resistance of composites and reduce their cost [4,5]. The effects of inorganic fillers on the strength and microstructure of PP composites are highly dependent on the particle shape and size distribution, agglomerate size, surface features, filler fraction and degree of dispersion [6].

Several researchers [7-9] confirmed the use of thermoplastic polymers grafted to maleic anhydride (MAH) as a compatibilizer to promote the compatibility of polymer blends and composites. As a result, the quality and performance of the PP composite was weakened. PP grafted with MAH is successful because

*Corresponding Author - E-mail: s.maou@univ-biskra.dz

it provides polarity and charge to the PP composite. At the same time, it helps the organic PP polymers to adhere to the inorganic materials [10].

Fuad et al. [11] used PP-*g*-MA as a compatibilizing agent. The MAH group on PP-*g*-MA interacts strongly with calcium carbonate, resulting in effective dispersion of $CaCO_3$ during the PP melting process.

One way to understand the link between the microscopic structure and macro characteristics of polymers is to explore the impact of residual stress (RS) induced by free quenching on the mechanical and structural properties of partially crystalline plastics [12], allowing for a better understanding of their relationship. Since the level of crystallinity attained by these polymers depends on their thermal properties, and the level of crystallinity determines their mechanical characteristics, such as rigidity, strength and resistance to force, the impact of thermal properties on polymers should be extensively investigated [2,13]. A fourth state may be formed following the rapid quenching of the iPP from the melt state and the widely recognized α, β, and γ crystallization changes [14,15].

Merabet et al. [16] studied the effect of cooling from a molten state on the strength and structure of iPP and concluded that cooling from the molten state to various temperatures decreased Izod impact strength values at every temperature studied. However, the degree of crystallinity attained by the polymer decreases at a temperature of 20°C. X-ray diffraction examination revealed that the α-structure dominates the main morphology of iPP. Recently, the impact of RS resulting from the free quenching approach on the thermophysical characteristics of polycarbonate (PC) and pure poly (methyl methacrylate) (PMMA) was examined by Barka et al. [17], who determined that quenching at temperatures greater than glass transition temperature (T_g) did not affect the heat transfer capacity or diffusivity of PC and PMMA. In contrast, heat transfer capacity and diffusivity decreased at temperatures lower than T_g (130°C). For example, consider the thermal conductivity of PC after annealing at 130°C, which shows that quenching can increase the insulating capacity of PC. These findings are consistent with those published in previous research studies on pigmented polycarbonate (PC/TiO_2) samples quenched under different temperatures [18]. Two ways to establish RS in polymers are available in the laboratory: irregular cooling (thermal quenching) and non-uniform plastic deformation (cold working). The term RS in this research context refers to those created using transitory heat gradients. Several efforts have evaluated residual stress' impact on the characteristics of molded polymers. Almost all polymer production procedures create residual tensions during processing. For example, variations in injection molding conditions may result in molecular orientation changes. Several researchers have employed free-quenching studies on materials [19,20], including semi-crystalline and amorphous polymers [21, 22] , to eliminate the influence of flow-driven orientation.

The goal of this research study is to examine the impact of quenching temperature and the $CaCO_3$ loading rate on the thermal and physical characteristics of PP/$CaCO_3$ composites, as well as enhance these characteristics.

EXPERIMENTAL

Raw materials

In this experiment, we utilized a commercial PP sourced from the Italian Company Himont, with a density of around 0.90 g/ml. Melting occurs at 165°C, with a melt index of 1.55 g/10 minutes at 230°C. Hermacarb 2FT is a treated micronized filler of extreme purity and cleanliness produced from $CaCO_3$ supplied by the Tunisian Society of Industrial Calcium Carbonate (STICC).

The dicumyl peroxide (DCP) (99% purity and molar mass 270 g/mol) and MAH (general formula $C_4H_2O_3$, molar mass 98g/mol, melting point 52.8°C, evaporation point 202°C) were supplied by Bayer (M) Ltd. of Cologne, Germany, MAH was used to produce the PP-*g*-MAH.

Preparation of PP-g-MAH

In an excess of acetone (100 ml), we dispersed the DCP (10 g) and the MAH (30 g); once the solution became homogeneous, the PP granules (80g) were impregnated while stirring (4 hours). The acetone was then evaporated at 70°C in an oven for 24 hours.

The grafting was carried out in the molten state in an internal mixer at 175°C and a screw speed of 40 rpm. The obtained product was subjected to grinding to be used.

First Quenching Process and Sample Preparation

Before being used, PP and $CaCO_3$ were dried for 24 hours in an oven at a temperature of 90°C. Melt mixing in a Brabender plastic order at a rotor speed of 60 rpm and 180°C was used to produce samples

Table 1. List of samples abbreviation and crystallinity (DSC).

samples	T (°C)	abbreviation	X_c
100 PP/4 PP-g-MAH/4 $CaCO_3$	Reference	C4	43.50
100 PP/4 PP-g-MAH/4 $CaCO_3$	0	C4.0	42.04
100 PP/4 PP-g-MAH/4 $CaCO_3$	40	C4.40	45.14
100 PP/4 PP-g-MAH/4 $CaCO_3$	80	C4.80	47.90
100 PP/4 PP-g-MAH/4 $CaCO_3$	air	C4.air	47.04
100 PP/4 PP-g-MAH/4 $CaCO_3$	annealing	C4.ann	51.62
100 PP/4 PP-g-MAH/8 $CaCO_3$	Reference	C8	45.70
100 PP/4 PP-g-MAH/8 $CaCO_3$	0	C8.0	43.12
100 PP/4 PP-g-MAH/8 $CaCO_3$	40	C8.40	46.28
100 PP/4 PP-g-MAH/8 $CaCO_3$	80	C8.80	52.43
100 PP/4 PP-g-MAH/8 $CaCO_3$	air	C8.air	52.05
100 PP/4 PP-g-MAH/8 $CaCO_3$	annealing	C8.ann	54.64
100 PP/4 PP-g-MAH/12 $CaCO_3$	Reference	C12	46.74
100 PP/4 PP-g-MAH/12 $CaCO_3$	0	C12.0	44.13
100 PP/4 PP-g-MAH/12 $CaCO_3$	40	C12.40	47.22
100 PP/4 PP-g-MAH/12 $CaCO_3$	80	C12.80	54.96
100 PP/4 PP-g-MAH/12 $CaCO_3$	air	C12.air	53.80
100 PP/4 PP-g-MAH/12 $CaCO_3$	annealing	C12.ann	56.93

with differing weight compositions, including PP/PP-g-MAH100/4 (this formulation is described as C) and inorganic filler $CaCO_3$ at 4, 8, and 12 phr, accordingly.

First Quenching Process

A granulator was used to produce pellets out of the C/$CaCO_3$ composite. Then, at a molding temperature of 180°C, the pellets were placed in a mold and compressed under 25 bars of pressure for 8 minutes. After being removed from the molds, the samples were subjected to a "first quench," in which they were cooled rapidly from molding temperature to room temperature over duration of 15 minutes.

Second Quenching Process

The samples molded at 180°C conducted a second round of free quenching in the air at the initial quenching temperature. These samples were heated for 2 hours at 130°C and cooled in water in the temperatures range of 0, 20, 30, 40, 50, 60, 70, and 80°C before being exposed to ambient conditions for 15 minutes. The term "second quench" describes this action. Samples used in this analysis are designated as C4, C8, and C12 (T denotes the quenching temperature).

Annealing Process

Finally, annealing is conducted so that a sample may be used as a standard. The air-quenched samples were used to produce annealed specimens. The samples were heated for 2 hours at 130°C before being cooled to room temperature at a rate of approximately 10°C every 30 minutes. The term "annealed samples" was named for these tests.

Characterization

Thermal characterizations

Differential scanning calorimetry (DSC)

Under an inert N_2 environment, a PE NELSON Differential Scanning Calorimeter model 1022 was used to examine the thermal behavior of composites (C4.T), (C8.T), and (C12.T). Using a heating rate of 10°C/min, we heated 4-7 mg samples from 40°C to 300°C. The enthalpy of melting (ΔH_m^0) and cold crystallization (ΔH_{cf}) were determined based on the heating curves to determine the crystallinity fraction χ_c, using Equation (1), where H_m^0 corresponds to 209 J/g and refers to the enthalpy of 100% crystalline PP [23].

$$\chi_c = (\Delta H_m - \Delta H_{cf}) / \Delta H_m^0 \quad (1)$$

Heat deflection temperature (HDT)

According to ASTM D648, the heat distortion temperature (HDT) was determined by heating a 3×13×127 mm^3 specimen in an oil bath at a rate of 2°C/min until the specimen distorted by 0.25 mm under 1.8 MPa. The data plot was created using the average of at least five separate tests performed on different samples.

Vicat softening temperature

To find out what temperature the material softens at, Vicat softening temperature tests (VST) were employed. A Zwick Vicat softening temperature tester set to 50 N force and 5°C/min heating rate was used to determine the temperature at which the indentor penetrates a depth of 1 mm into the sample. The data plot was created using the average of at least five separate tests performed on different samples.

Mechanical characterizations

Tensile test

Dumbbell-shaped specimens of 115 mm in length, 13 mm in width, and 20 mm in gauge length were used to determine the tensile characteristics. A universal testing machine with a crosshead speed of 10 mm/min was used to conduct the tests. All tests were conducted in conformity with ASTM D638-72. The tensile characteristics (modulus of elasticity and elongation-at-break) of the quenched specimens were calculated from their stress-strain curves. The average results from testing five samples were used to generate the graph.

Notched Izod impact strength

The flexural shock resistance of a specimen is measured by the energy required to break a standard specimen when impacted by a standardized pendulum hammer installed in a standard machine. At room temperature, ASTM D256-73 in accordance impact strength parameters of Izod were evaluated using a CEAST 6546/000 machine equipped with a 15 J pendulum and 3×12.7×63 mm^3 specimens. Some of the molds used had notches with a radius of 0.5 mm. Others have a notch drilled into them with a 0.5 mm radius. The notch's apex is inside the residual compressive zone owing of the carefully selected radius. The data plot was created using an average of at least five separate tests performed on different samples.

Microhardness measurements

At room temperature, a Leitz (Wetzlar, Germany) micro indentation with a diamond indenter on a square base was used to determine the microhardness (H). Penetration redirected the value of (H) away from the remaining area. Each sample's surface was indented eight times, and the mean of those readings was plotted.

Physical characterization

Density measurement

Filling the pycnometer to the mark on its neck or to the top edge of a capillary tube, according to the pycnometer's nominal volume, and then weighing the material allows one to calculate its density. Measurement of density using pycnometer is preferred because of its extreme precision (to 10-5 g/cm^3). The data plot was drawn using the mean value from at least five samples.

m_1: mass of the pycnometer full of liquid

m_2: mass of the sample alone

m_3: mass of the pycnometer full of liquid with the sample immersed in it

Where the mass of the liquid is expressed by:

$m_{liquid} = r_{liquid} V_{sample} = r_{liquid} (m_{sample} / r_{sample}) = r_{liquid} (m_2 / r_{sample})$

From the combination of these equations we derive the final density of the sample:

$$\rho_{sample}(t) = \frac{m_2}{m_1 + m_2 - m_3} \times \rho_{liquid}(t) \quad (2)$$

$$d^{t}_{t_0} = \frac{m_2}{m_1 + m_2 - m_3} \times \frac{\rho_{liquid}(t)}{\rho_{water}(t_0)} \quad (3)$$

RESULTS AND DISCUSSION

Elongation-at-fracture and Impact strength

The notched and unnotched Izod impact strength (ak) and (an) as a function of cooling down temperature for $C/CaCO_3$ samples (first cooled in air) is depicted in Figures 1 and 2, respectively. The measured values of Izod impact strength reach their highest at 0°C for the cooling temperature. Alternatively, one can observe that the Izod impact strength (ak) and (an) values decrease as the cooling temperature increases. As an example, the Izod impact strength (ak) of unnotched specimens decreases from (29.375; 28.175 and 27.275 kJ/m^2) to (21.300; 20.000 and 19.000 kJ/m^2) at quenching temperatures varying from 0°C to 80°C for a molding temperature of 180°C. The differences are more pronounced for annealed samples (18.72; 18.02 and 17.43 kJ/m^2 for C4, C8, and C12, respectively). The crystalline state that develops during thermal treatment influences the impact resistance of semi-crystalline polymers filled with $CaCO_3$. As the impact resistance decreases, the crystallinity of the material increases, the elongation-at-fracture as a function of the cooling temperature is depicted in Figure 3. At a temperature of 0°C, the maximal elongation-at-break is obtained, which is again associated with satisfactory flexibility under these conditions. The elongation-at-break values decrease considerably as the cooling temperature increases.

The drop in impact resistance and strain-at-break depicted in Figures 1,2 and 3, respectively, are associated with a ductile-brittle variation in the behavior of $PP/CaCO_3$, our results correlate with the works of Piekarska et al. [24].

An increase in free volume was confirmed using

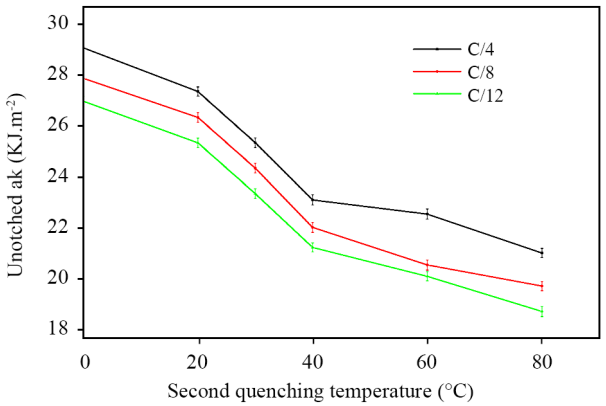

Figure 1. Impact strength of unnotched Izod C4, C8, and C12 as a function of second cooling temperature.

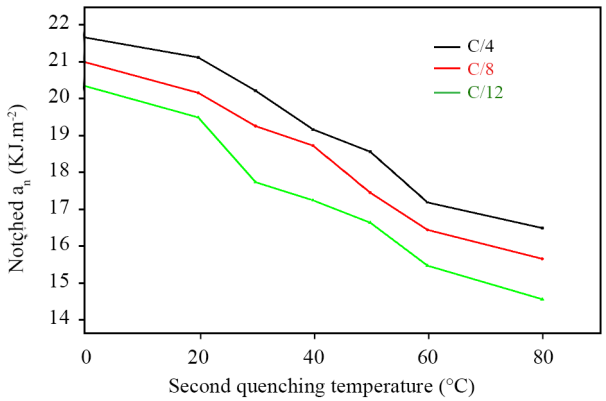

Figure 2. Impact strength of notched Izod C4, C8 and C12 as a function of the second cooling temperature.

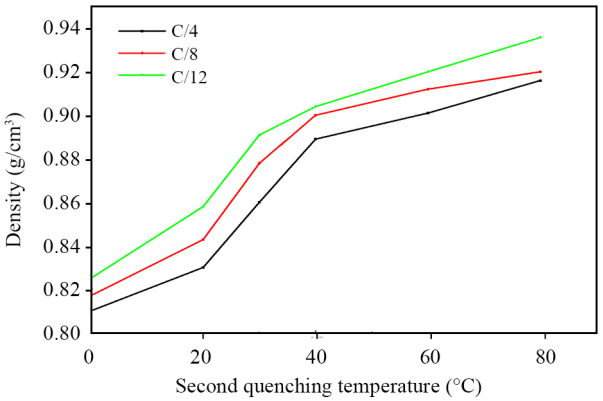

Figure 4. C4, C8 and C12 density as a function of the second cooling temperature.

density measurements. The results are displayed in the following section. Since the impact strength depends on the capacity of polymer chains to conduct segmental mobility and dissipate the energy that causes fracture propagation, an increase in free volume may also be causing the increase in impact strength.

Density, microhardness, and Young's modulus

Figures 4, 5, and 6 depict the variations in density, microhardness and Young's modulus as a function of the second cooling temperature. Density measurements provide an indication of the composite samples' coarse molecular adjustments. When the density of a crystalline material decreases, so does its crystallinity and vice versa. As the second cooling temperature increases, the density, microhardness and Young's modulus increase notably. In the case of rapid cooling, corresponding to a second cooling temperature of 0°C, there is less time for the reorganization of macromolecules. As a consequence, the density, microhardness, and modulus of elasticity all drop as the free volume rises. It has also been noted that the rate of temperature change and the stress induced by heat govern the free volume (and hence the density) [12, 25].

As stated by Van Krevelen, density (ρ) is correlated with Young's modulus (E): i.e., samples with a lower density also have a lower Young's modulus [26]. Annealing increases the density, microhardness and crystallinity of a material. Notably, the samples cooled for a second time at 0°C typically have a lower density, microhardness, modulus of elasticity, and crystallinity than those cooled in air for the second time. Alternatively, annealing exhibits a substantial increase in the modulus of C4, C8 and C12 (2550-2390 MPa) compared with the cooled material (2260 MPa to 1480 MPa), which is caused by the dramatic improvement in crystallinity brought on by the heating process. However, thermal residual stresses are mostly removed during annealing, suggesting that the higher modulus values seen after annealing are due to a reduction in structural stresses [27].

Samples cooled at high temperatures are usually stronger than rapidly cooled samples. This is especially true because structural stresses boost crystallinity.

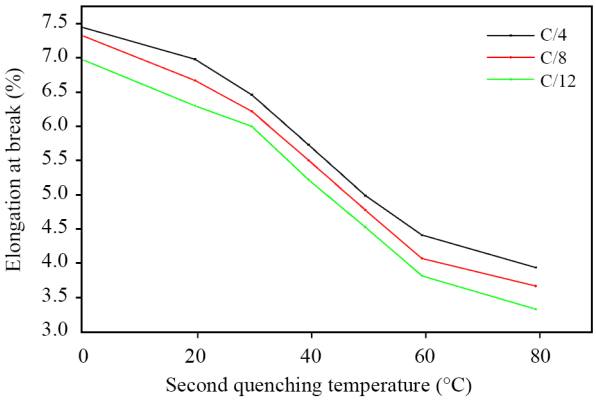

Figure 3. Elongation-at-break of C4, C8 and C12 as a function of the second cooling temperature.

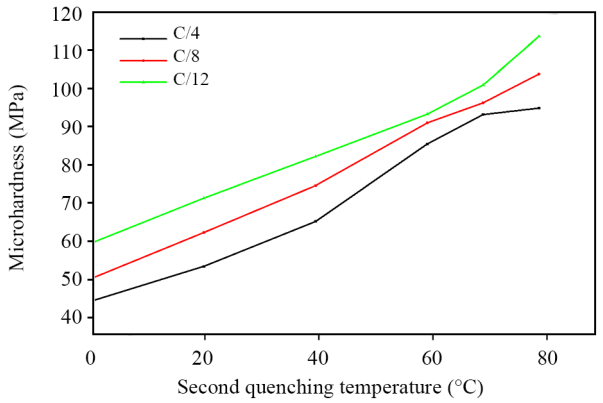

Figure 5. Microhardness of C4, C8 and C12 as a function of the second cooling temperature.

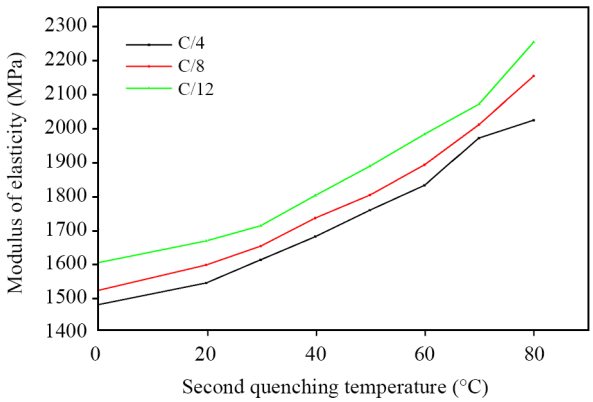

Figure 6. Elastic modulus of C4, C8 and C12 as a function of the second cooling temperature.

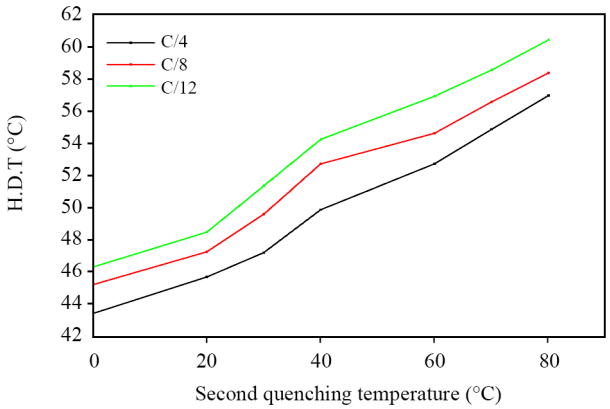

Figure 8. Temperature of thermal distortion for C4, C8 and C12 as a function of the second cooling temperature.

VST, HDT and DSC

The Vicat softening point decreases in response to an increase in compressive stresses. Additionally, it remains sensitive to free volume, which facilitates the physical gliding of segmented molecules. Figure 7 depicts the variations in VST as a function of the second cooling temperature for C4, C8 and C12 samples. A low second cooling temperature is observed to reduce the VST. This is because the compressive stresses and free volume are greater at this cooling temperature.

As observed for Young's modulus, Vicat softening point, and density, the HDT decreases as the second cooling temperature decreases (Figure 8). Since tensile stresses increase, the total tensile tension applied to the HDT specimen decreases when tensile stresses are present in the specimen. Consequently, the HDT evolves similarly to the Vicat softening point.

Parambil et al. [28] did not measure the variation in free volume and suggested that the increase in HDT correlated to a decrease in free volume due to the relaxation of thermal stresses and molecular direction. As HDT and density vary in the same manner, the evolution of HDT may also be partly attributable to the evolution of free volume due to the various thermal treatments.

The thermograms of the C4, C8 and C12 composites as a function of the second cooling temperature are depicted in Figures 9 through 11. Thermal experiments can produce vastly different results depending on the variation in the second cooling temperature and of the filler $CaCO_3$ weight fraction.

When modifying the second cooling temperature or quantity of $CaCO_3$, T_g, T_m, H_m, the degree of crystallinity (χ_c) also changes. In all cooled composites, an increase in crystallization and a significant increase in the melt temperature, T_m, was observed as a function of the second cooling temperature.

The thermograms in Figures 9-11 demonstrate that the highest degree of crystallinity is obtained with annealed composites and specimens cooled for a second time at 80°C and is consequently greater than the other degrees of crystallinity of specimens cooled at various temperatures.

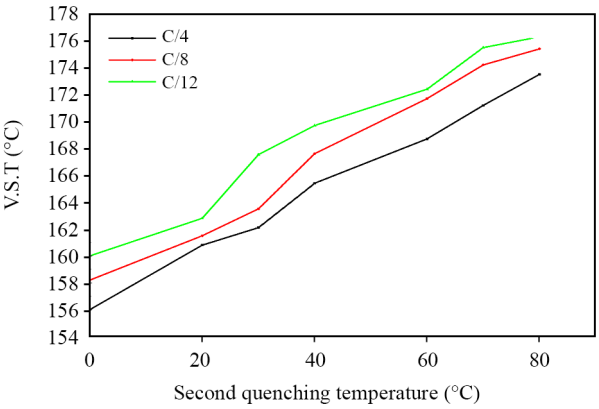

Figure 7. VSTs for C4, C8 and C12 as a function of the second quenching temperature.

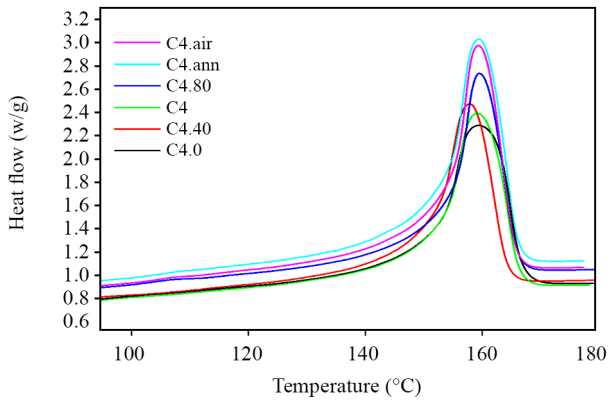

Figure 9. Thermograms of C4 as a function of the second cooling temperature.

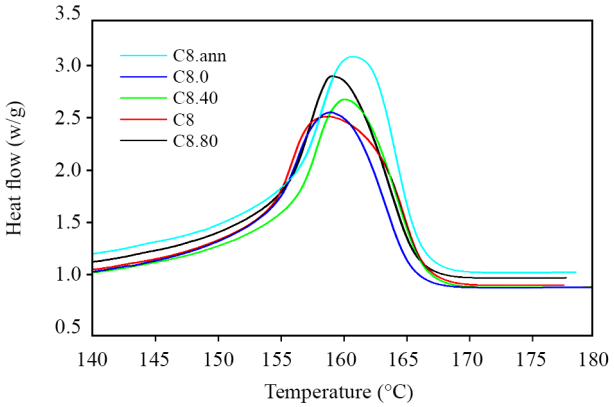

Figure 10. Thermograms of C8 as a function of the second cooling temperature.

Effect of $CaCO_3$

Figures 1, 2, and 3 show that the greatest values of impact strength and elongation-at-break of PP/$CaCO_3$ composites are observed for the C4 formulation, corresponding to a rate of 4 wt.% of $CaCO_3$ and rapid cooling (0°C). We note that by keeping the same quenching temperature (0°C) and by increasing the $CaCO_3$ loading for the C8 and C12 formulations, the impact resistance and elongation-at-break of these composites decrease. Figures 4-8 indicate that the density, microhardness, elastic modulus, TFC, and HDT of the PP/$CaCO_3$ composites reach their lowest values at rapid cooling (0°C) and for the C4 formulation containing 4 wt.% of $CaCO_3$. At the same quenching temperature (0°C), by increasing the charge rate for the C8 and C12 formulations, an increase in these properties is envisaged. This can be explained by an increase in the crystallinity rate of the composites studied (see figures 9-11), given that the $CaCO_3$ particles have the role of nucleation agents. Effect of cooling down from 130°C to the controlled temperature [29].

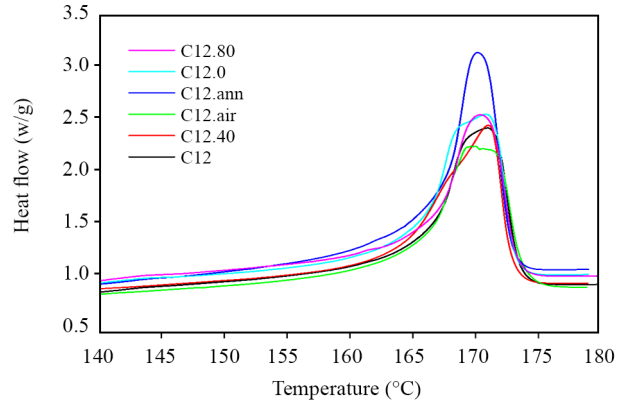

Figure 11. Thermograms of C12 as a function of the second cooling temperature.

CONCLUSION

Using mechanical, physical, and thermal measurements, the impact of quenching on the thermophysical behaviours of PP/$CaCO_3$ was studied. When $CaCO_3$ is added to PP, the modulus of elasticity, density, microhardness, VST, and HDT decreases while the Izod impact strength and elongation-at-break decrease. The fillers function as a material's default, starting the breaking process in mechanical tests. It has been demonstrated that greater ductility can be obtained by quenching samples from 130°C to 0°C. This quenching provides greater residual strain as well as free volume, which raises the Izod impact strength value and elongation-at-fracture while reducing the modulus of elasticity. The minimal density reached after cooling from 130°C to 0°C was associated with a larger quantity of free volume, leading to increased molecular mobility.

The material's thermal history significantly impacts the evolution of residual stresses, which in turn alter material properties. To enhance their mechanical characteristics, composites may be subjected to a simple and efficient procedure known as heat quenching.

ACKNOWLEDGEMENTS

The authors extend their appreciation to the Ferhat Abbas University, Setif, Algeria for funding this work.

CONFLICTS OF INTEREST

The authors declare that they have no conflicts of interest.

REFERENCES

1. Essabir H, Raji M, Laaziz SA, Rodrique D, Bouhfid R, Qaissa A (2018) Thermo-mechanical performances of polypropylene biocomposites based on untreated, treated and compatibilized spent coffee grounds. Compos Part B Eng 149: 1-11

2. Latreche L, Haddaoui N, Cagiao ME (2017) Calcium carbonate, kaolin and silica filled polypropylene/polystyrene blends: Influence of free quenching. Rev Roum Chim 62: 267-276
3. Karian H (2003) Automotive applications for polypropylene and polypropylene composites. In: Handbook of polypropylene and polypropylene composites, revised and expanded (pp. 592-600), CRC Press
4. Al-Samhan M, Al-Attar F (2022) Comparative analysis of the mechanical, thermal and barrier properties of polypropylene incorporated with $CaCO_3$ and nano $CaCO_3$. Surf Interfaces 31: 102055
5. Maou S, Meftah Y, Meghezzi A (2023) Synergistic effects of metal stearate, calcium carbonate, and recycled polyethylene on thermo-mechanical behavior of polyvinylchloride. Polyolefins J 10: 1-11
6. Palanikumar K, AshokGandhi R, Raghunath BK, Jayaseelan V (2019) Role of calcium carbonate($CaCO_3$) in improving wear resistance of polypropylene(PP) components used in automobiles. Mater Today Proc 16: 1363-1371
7. Maou S, Meftah Y, Tayefi M, Meghezzi A, Grohens Y (2022) Preparation and performance of an immiscible PVC-HDPE blend compatibilized with maleic anhydride (MAH) via in-situ reactive extrusion. J Polym Res 29: 161
8. Maou S, Meftah Y, Grohens Y, Kervoelen A, Magueresse A (2023) The effects of surface modified date-palm fiber fillers upon the thermo-physical performances of high density polyethylene-polyvinyl chloride blend with maleic anhydride as a grafting agent. J Appl Polym Sci 140: e53781
9. Looijmans SF, Cavallo D, Merino DH, Martinez JC, Anderson PD, Breemen LC (2023) Shear-induced structure formation in MAH-*g*-PP compatibilized polypropylenes. Macromolecules 56: 5278-5289
10. Yang N, Zhang ZC, Ma N, Liu HL, Zhan XQ, Li B, Gao W, Tsai FC, Jiang T, Chang CJ, Chiang TC, Shi D (2017) Effect of surface modified kaolin on properties of polypropylene grafted maleic anhydride. Results Phys 7: 969-974
11. Fuad MYA, Hanim H, Zarina R, Ishak ZAM, Hassan A (2010) Polypropylene/calcium carbonate nanocomposites - effects of processing techniques and maleated polypropylene compatibiliser. Express Polym Lett 4: 611-620
12. Vargas-isaza C, Posada-correa J, León JB (2023) Analysis of the stress field in photoelasticity used toevaluate the residual stresses of a plastic injection-molded part. Polymers (Basel) 15: 3377
13. Latreche L, Rouabah F, Haddaoui N, (2019) Influence of free quenching on mechanical physical and thermal properties of high density polyethylene. Chem Process Eng Res 59: 15-21
14. Zhao J, Wang Z, Niu Y, Hsiao BS, Piccarolo S (2012) Phase transitions in prequenched mesomorphic isotactic polypropylene during heating and annealing processes as revealed by simultaneous synchrotron SAXS and WAXD technique. J Phys Chem B 116: 147-153
15. Mollova A, Androsch R, Mileva D, Gahleitner M, Funari SS (2013) Crystallization of isotactic polypropylene containing beta-phase nucleating agent at rapid cooling. Eur Polym J 49: 1057-1065
16. Merabet S, Rouabah F, Fois M (2019) Heat treatment of isotactic polypropylene: The effect of free quenching from the melt state. Int J Polym Anal Charact 24: 313-325
17. Barka B, Rouabah F, Zouaoui F, Fois M, Nouar Y, Bencid A (2022) Thermophysical behavior of polycarbonate: Effect of free quenching above and below the glass transition temperature. Adv Mater Res 1174: 123-136
18. Rouabah F, Fois M, Ibos L, Boudenne A, Dadache D, Haddaoui N (2007) Mechanical and thermal properties of polycarbonate. II. Influence of titanium dioxide content and quenching on pigmented polycarbonate. J Appl Polym Sci 106: 2710-2717
19. Kahmann S, Nazarenko O, Shao S, Hordiichuk O, Kepenekian M, Even J, Kovalenko MV, Blake GR, Loi MA (2020) Negative thermal quenching in FASnI3 perovskite single crystals and thin films. ACS Energy Lett 5: 2512–2519
20. Srinivasan V, Hasainar H, Singh TN (2022) Experimental study on failure and fracturing attributes of granite after thermal treatments with different cooling conditions. Eng Geol 310: 106867
21. Guo X, Isayev AI (2000) Thermal residual stresses in freely quenched slabs of semicrystalline polymers: Simulation and experiment. J Appl Polym Sci 75: 1404-1415
22. Fayolle B, Richaud E, Colin X, Verdu J (2008) Degradation-induced embrittlement in semi-

crystalline polymers having their amorphous phase in rubbery state. J Mater Sci 43: 6999-7012
23. Latreche L, Haddaoui N, Cagiao ME (2016) The effect of various compatibilizers on thermal, mechanical, and morphological properties of polystyrene/polypropylene blends. Russ J Appl Chem 89: 1713-1721
24. Piekarska K, Piorkowska E, Bojda J (2017) The influence of matrix crystallinity, filler grain size and modification on properties of PLA/calcium carbonate composites. Polym Test 62: 203-209
25. Guevara-Morales A, Figueroa-López U (2014) Residual stresses in injection molded products. J Mater Sci 49: 4399-4415
26. Van Krevelen DW (1972) Properties of polymers. Elsevier, Amsterdam
27. Danielsen SPO, Beech HK, Wang S, El-Zaatari BM, Wang X, Sapir L Ouchi T, Wang Z, Johnson PN, Hu Y, Lundberg DJ, Stoychev G, Craig SL, Johnson JA, Kalow JA, Olsen BD, Rubinstein M (2021) Molecular Characterization of Polymer Networks. Chem Rev 121: 5042-5092
28. Parambil NK, Chen BR, Deitzel JM, Gillespie JW (2022) A methodology for predicting processing induced thermal residual stress in thermoplastic composite at the microscale. Compos Part B Eng 231: 109562
29. Doufnoune R, Haddaoui N, Riahi F (2006) Elaboration and characterization of an organic/inorganic hybrid material: Effect of the interface on the mechanical and thermal behavior of PP/$CaCO_3$ composite. Int J Polym Mater 55: 815-835